RESEARCH ARTICLE

Editorial Process: Submission:31/01/2026 Acceptance:05/09/2026 Published:28/09/2026

α-Chaconine as a Potential Inhibitor of Mutant Phosphatidylinositol 3-Kinase Alpha in Breast Cancer Stem Cells: Insights from Structure Prediction and Molecular Dynamics

Bakti Wahyu Saputra[1,2], Navista Sri Octa Ujiantari[3], Badra Sanditya Rattyananda[4,5], Ratna Surya Alwi[6], Agustina Setiawati[7], Adam Hermawan[2,8]*

Abstract

Introduction: Breast cancer stem cells (BCSCs) promote chemoresistance and metastasis by activating aberrant signaling pathways such as phosphatidylinositol 3-kinase/protein kinase B (*PI3K/Akt*). α-Chaconine (CHA) is a steroidal glycoalkaloid that has demonstrated cytotoxic and antiproliferative activity in various cancer models, possibly through modulation of the *PI3K/Akt* pathway. However, its direct interaction with *PI3Kα* and related alterations has not yet been elucidated. This study aimed to assess CHA as a potential BCSC-targeting agent, particularly as a PI3K inhibitor targeting both wild-type and mutant *PI3Kα*, using an *in silico* approach. **Methods:** Mutation data were retrieved from cBioPortal and analyzed using MutPred2. SWISS-MODEL was used to generate homology models of the wild-type and mutant *PI3Kα* structures. Structural validation was performed using PROCHECK and ERRAT. Molecular docking was employed to evaluate the binding affinity of the *PI3Kα*-CHA complex. Molecular dynamics simulations were conducted to assess the stability of the interaction between CHA and *PI3Kα*. **Results:** Three *PIK3CA* mutations were identified as pathogenic: *E542K, E545K*, and *H1047R*. Molecular docking revealed a strong binding affinity of alpelisib to both wild-type and mutant (*E542K, E545K*, and *H1047R*) forms of p110 α. CHA exhibited the lowest binding energy with the *H1047R* mutant, with a docking score of −9.93 kcal/mol. Molecular dynamics simulations demonstrated stable interactions of alpelisib with wild-type, *E542K*, and *E545K* mutants, whereas CHA showed stable interaction only with the *H1047R* mutant. MM-PBSA calculations confirmed the lowest binding free energies for alpelisib-wild-type p110α and CHA-H1047R complexes, with values of −29.21 kcal/mol and −25.88 kcal/mol, respectively. **Conclusion:** These findings provide a basis for further *in vitro* and *in vivo* studies to evaluate CHA as a selective PI3K inhibitor targeting the *H1047R PIK3CA* mutation in breast cancer stem cells.

Keywords: breast cancer stem cells, alpha-chaconine, phosphatidylinositol 3-kinase alpha, mutation, anticancer

Asian Pac J Cancer Prev, **27 (9)**, 3411-3419

Introduction

Breast cancer is the second leading cause of death among women globally. In 2023, the number of women diagnosed with breast cancer was estimated at 2.3 million cases, according to a World Health Organization report. Several treatments, including chemotherapy, surgery, radiation, and immunotherapy, are used to eliminate breast cancer cells [1]. However, treatment failure has been associated with cancer cell progression, resistance, and metastasis [2]. Chemotherapy resistance and metastasis are partly driven by breast cancer stem cells (BCSCs), which possess stem cell-like self-renewal and differentiation capabilities [3]. BCSCs also exhibit aberrant activation

*[1]Master in Pharmaceutical Sciences, Faculty of Pharmacy, Gadjah Mada University, Yogyakarta 55281, Indonesia. [2]Laboratory of Advanced Pharmaceutical Sciences, Faculty of Pharmacy, Universitas Gadjah Mada, Sekip Utara II, 55281, Yogyakarta, Indonesia. [3]Laboratory of Medicinal Chemistry, Department of Pharmaceutical Chemistry, Faculty of Pharmacy, Universitas Gadjah Mada, Sekip Utara II, 55281, Yogyakarta, Indonesia. [4]Research Centre for Computation, Research Organization for Electronics and Informatics, National Research and Innovation Agency (BRIN), Jl. Tamansari 71, Bandung City, 40132, Indonesia. [5]Doctoral Program of Computational Science, Division of Mathematical & Physical Sciences, Graduate School of Science & Technology, Kanazawa University, Kakuma, Kanazawa, Ishikawa, 920-1192, Japan. [6]Research Centre for Computing, National Research and Innovation Agency (BRIN), Jl. Raya Jakarta-Bogor KM 46 Cibinong, 16911, Indonesia.[7]Faculty of Pharmacy, Sanata Dharma University, Paingan, Maguwoharjo, Depok, Sleman, Yogyakarta, 55282, Indonesia. [8]Laboratory of Macromolecular Engineering, Department of Pharmaceutical Chemistry, Faculty of Pharmacy, Universitas Gadjah Mada Sekip Utara II, 55281, Yogyakarta, Indonesia. *For Correspondence: adam_apt@ugm.ac.id*

of various signaling pathways, including interleukin-6/signal transducer and activator of transcription 3, phosphatidylinositol 3-kinase/protein kinase B (*PI3K/Akt*), and Notch [4, 5]. Thus, BCSC-targeted therapy is crucial for improving chemotherapy outcomes.

The *PI3K/Akt* pathway is regulated by the catalytic *PI3Kα* enzyme, which facilitates the phosphorylation of phosphatidylinositol 4,5-bisphosphate to phosphatidylinositol 3,4,5-triphosphate using ATP and activates downstream signaling pathways related to cancer, including Akt and mechanistic target of rapamycin [6]. *PI3Kα* comprises a catalytic subunit (p110α) and a regulatory subunit (p85α), encoded by the *PIK3CA* and PIK3R1 genes, respectively. Phosphoinositide 3-kinase catalytic subunit alpha (*PIK3CA*) is one of the most frequently mutated genes involved in abnormal activation of the *PI3K/Akt* pathway [7]. Due to its critical role in cancer progression, *PI3Kα* has emerged as an important therapeutic target. Currently, several PI3K inhibitors have been developed for cancer therapy, such as alpelisib, inavolisib, and taselisib. Alpelisib has demonstrated clinical efficacy in various *PIK3CA* mutations [8]. Inavolisib (GDC-0077) is advancing into Phase III clinical trials for breast cancer treatment [9]. Taselisib has shown improved efficacy and tolerability in clinical trials involving patients with *PIK3CA* mutations [10]. Despite significant advances in the development of PI3K inhibitors, limitations such as adverse effects (including hyperglycemia, rash, and diarrhea) and drug resistance persist [11]. Consequently, there is a continued need to identify more effective and selective *PI3Kα* inhibitors for various PI3K mutants.

The use of phytochemical compounds for breast cancer therapy has recently emerged as a promising approach. One such compound, α-chaconine (CHA), is a glycoalkaloid compound found in potatoes. CHA has been shown to induce apoptosis, inhibit ERK signaling, and activate caspase-3 in HT-29 colon carcinoma cells [12]. Combined treatment with CHA and trastuzumab reduces HCC1954-TRZ cell viability and increases sensitivity to trastuzumab [13]. CHA has also been reported to decrease metastasis in A549 lung cancer cells via the *PI3K/Akt* signaling pathway [14] and to reduce Akt and estrogen receptor alpha expression in RL-95-2 endometrial cancer cells [15]. These findings suggest CHA's potential as a *PI3Kα* inhibitor. However, the interaction of CHA with the *PI3Kα* structure and its effects on different *PI3Kα* mutants have not yet been explored. Therefore, this study investigates the inhibitory effect of CHA on *PI3Kα*.

Nowadays, bioinformatics approaches are widely employed to accelerate pharmaceutical research, including mutant prediction and molecular dynamics simulation. Mutant prediction is used to assess the impact of mutations on protein stability, which plays a major role in disease pathogenesis [16]. In this study, we aimed to investigate the CHA interactions with mutated *PI3Kα* using an in silico approach. *PIK3CA* mutations in breast cancer were identified using cBioPortal, and the mutation data were analyzed using Mutpred2 to identify structural and functional alterations. The wild-type and mutant p110α structures were modeled using SWISS-MODEL and evaluated using PROCHECK and ERRAT. Molecular docking was performed to predict the interaction between candidate compounds and target proteins. Molecular dynamics simulations were conducted to assess the stability of the protein-ligand complex over time, playing a crucial role in predicting the stability of the protein-ligand complex [17].

Materials and Methods

Identification of PIK3CA mutations

Major mutations in *PIK3CA* were identified through cBioPortal (https://www.cbioportal.org/) [16]. The *PIK3CA* gene was queried within breast cancer studies. The top three mutations with the highest frequency among patients were selected for further structural and functional prediction analysis using Mutpred2 (https://mutpred.mutdb.org/). A threshold of 0.5 was used to classify the variants: scores greater than 0.5 were considered disease-associated, whereas scores less than 0.5 were considered benign [18, 19].

Three-dimensional modeling of proteins

The *PIK3CA* amino acid sequences (Uniprot ID: P42336) were retrieved from the Uniprot database (https://www.uniprot.org/). The three-dimensional (3D) structure of the protein was generated using the SWISS-MODEL homology-modeling server (https://swissmodel.expasy.org) [20]. The modeled protein structure was superimposed onto the crystal structure of 2RD0 using UCSF Chimera to assess similarity with the experimental structure.

Protein evaluation

Validation of the SWISS-MODEL-generated 3D structure was performed using PROCHECK and ERRAT tools available on the SAVES v6.0 server (https://saves.mbi.ucla.edu/) [21, 22]. PROCHECK evaluates stereochemical quality through Ramachandran plot analysis, while ERRAT assesses non-bonded atomic interactions to identify potential structural errors.

Molecular docking

The ligand structure was obtained from the PubChem database and converted into a 3D structure using Marvin Sketch. The ligand and protein structures were prepared for molecular docking using BIOVIA Discovery Studio 2024 by adding hydrogen atoms and assigning charges. AutoDock Tools 1.5.7 was used for docking, with grid box coordinates set at x = 60.737, y = 58.566, and z = 112.281, and a grid size of 40 × 40 × 40 Å, as determined in a previously published study [23]. Molecular docking was performed to evaluate ligand-PI3K interactions and estimate binding free energy.

Molecular dynamics simulations

GROMACS 2024.4 was used to perform molecular dynamics (MD) simulations on protein-ligand complexes obtained from molecular docking. The CHARMM36 force field was applied to parameterize both protein and ligand properties. The pdb2gmx tool was used to generate the

topology of p110α, while ligand topology was obtained using the CHARMM General Force Field (CGenFF) server (https://cgenff.com/) [22]. All protein-ligand systems were placed at the center of a dodecahedron box and solvated using the simple point charge water model. The charge of the p110α system was neutralized by adding appropriate sodium and chloride ions. Energy minimization was then performed over 50,000 steps to gradually relax the systems. The systems were equilibrated under NVT (constant number, volume, temperature) and NPT (constant number, pressure, temperature) ensembles for 1 nanosecond (ns) at 310 K using a Berendsen thermostat and maintained at 1 bar pressure. Short-range interactions were calculated using a force-switch cutoff of 1.2 nm during energy minimization and equilibration phases. Long-range electrostatic interactions were treated using the Particle-Mesh-Ewald (PME) algorithm, and hydrogen bonds were constrained using the Linear Constraint Solver (LINCS) algorithm. Subsequently, 100-ns MD simulations were performed without constraints using a 2 fs integration time step, with trajectory snapshots saved every 1 ps. The MD trajectories were analyzed using parameters including root-mean-square deviation (RMSD), root-mean-square fluctuation (RMSF), solvent-accessible surface area (SASA), and radius of gyration (Rg). The gmx_MMPBSA was employed to assess the binding affinity of the complexes [24].

Results

Identification of PIK3CA mutations

Genetic alterations of *PIK3CA* in breast cancer were analyzed using cBioPortal. *PIK3CA* was used as the query gene symbol and analyzed across breast cancer studies available in cBioPortal. The breast cancer (MSK, Nature Cancer 2020) study exhibited an alteration frequency of 80% in a population with significant mutations (Figure 1A). Across all studies, mutations were the dominant type of alteration in breast cancer patients, and they were further analyzed to determine mutation location and frequency. Figure 1B illustrates the mutation profile and its location within the protein domain, while Table 1 presents the number of patients for each mutation, with a total of 15,927 patients. Among *PIK3CA* mutations, the *H1047R* mutant was the most prevalent, identified in 1,264 patients, followed by *E545K* (675 patients) and *E542K* (385 patients). The three most frequent mutations were subsequently submitted to the Mutpred2 server. Supplementary Table 1 shows the prediction scores for these mutations (*E542K*, *E545K*, and *H1047R*), all of which were classified as "disease." Thus, the "disease" status indicates that the amino acid alteration is recognized as pathogenic.

Table 1. Frequency of *PIK3CA* Mutations in Breast Cancer Patients According to cBioPortal Studies

Mutation	Frequency
H1047R	1264
E545K	675
E542K	385

Three-dimensional modeling and evaluation of proteins

This study aimed to evaluate the potential of CHA as a *PI3Kα* inhibitor in both wild-type and mutant forms. Homology modeling was employed due to the lack of experimentally resolved structures for p110α mutants. The p110α structures were generated using SWISS-MODEL and superimposed onto the crystal structure of 2RD0 (Figure 1C). The results were evaluated using the PROCHECK web-based program to generate Ramachandran plots and assess the energetically feasible regions of the p110α model and the ERRAT web server to assess the overall quality factor. Ramachandran plots for the wild-type and mutant p110α structures are presented in Supplementary Figure 1A–D. The quality of 3D structures of *PIK3CA* was further validated using both Ramachandran analysis and ERRAT (Supplementary Table 2). In the Ramachandran plot of the wild-type, *E542K*, and *E545K* p110α mutant, 92.8% of residues were located in the most favorable regions, while 7.0% and 0.2% were found in additionally allowed territories and regions, respectively. Notably, no residues (0.0%) were present in disallowed regions. These findings indicate strong structural integrity of the p110α models.

Molecular docking

Molecular docking was performed using AutoDock 4.2 to evaluate the binding affinities of alpelisib and CHA with p110α in wild-type and hotspot mutants, including *E542K*, *E545K*, and *H1047R*. The results (Table 2) showed variations between wild-type and mutant models. The conventional *PI3K* inhibitor alpelisib exhibited a binding energy of −10.29 kcal/mol with wild-type p110α, forming hydrogen bonds with Lys802, Val851, Ser854, and Gln859 residues. For the mutant p110α, the binding energies were −10.21 kcal/mol (*E542K*), −10.38 kcal/mol (*E545K*), and −10.27 kcal/mol (H1047R), with hydrogen bonding primarily involving Val851, Ser854, and Gln859 residues. The binding interactions of alpelisib with wild-type and mutant p110α are shown in Supplementary Figure 2A–D.

For CHA, the binding energies were −8.36 kcal/mol (wild-type), −8.55 kcal/mol (*E542K*), −9.08 kcal/mol (*E545K*), and −9.93 kcal/mol (H1047R). The CHA-wild-type p110α complex formed hydrogen bonds with Arg770, Ser773, Ser919, and Asp933 residues. In mutant complexes, hydrogen bonds were observed with Lys802 and Tyr836, along with additional interactions: Asp810 (*E542K*), Ala775 (*E545K*), and Ser774, Ser919, and Asp933 (H1047R). The 2D binding interactions between CHA and wild-type and mutant p110α are presented in Supplementary Figure 2E-H, while a comparison of 3D structures for the alpelisib-wild-type and CHA-H1047R complexes is shown in Supplementary Figure 3A-B.

Molecular dynamics simulations

MD simulations were performed over 100 ns to evaluate the stability of interactions between CHA or alpelisib and wild-type, *E542K*, *E545K*, and *H1047R* mutants of p110α. Several parameters were evaluated, including RMSD, RMSF, SASA, and Rg. The RMSD of ligand-to-backbone was calculated to assess ligand movement within the binding site (Figure 2A and 2B). Alpelisib demonstrated

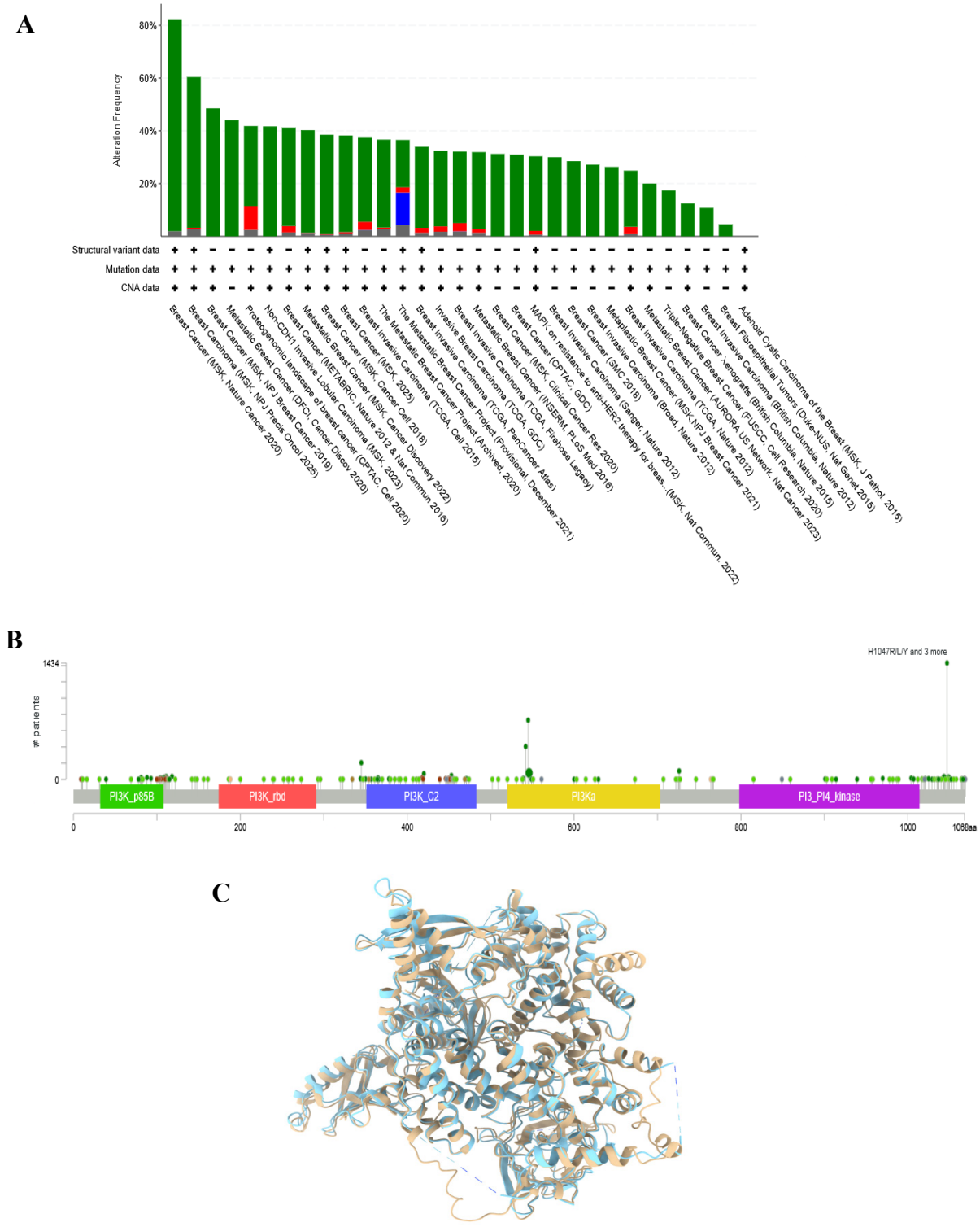

Figure 1. Genetic Alteration Analysis of *PIK3CA* in Breast Cancer Studies from cBioPortal. (A) Summary of alterations in PIK3CA across breast cancer studies in cBioPortal. (B) Mutation profiles of PIK3CA across breast cancer studies in cBioPortal. (C) Superimposition of the modeled p110α (yellow) with the crystal structure of p110α (protein Data Bank ID: 2RD0; cyan).

stable conformations in wild-type, *E542K*, and *E545K* complexes, with RMSD values below 5 Å throughout the simulation (Figure 2A). However, the alpelisib-H1047R complex exhibited fluctuating RMSD values after 80 ns, indicating conformational instability. In contrast, CHA exhibited high RMSD fluctuations (up to 25 Å) in wild-type, *E542K*, and *E545K* complexes (Figure 2B), whereas the CHA-H1047R complex remained stable, with RMSD values below 5 Å over a 100-ns simulation, indicating selective and stable interaction with the *H1047R* mutant. RMSF analysis was conducted to evaluate the fluctuation of amino acid residue in p110α (Figure 2C and 2D). The alpelisib-*E542K* complex showed notable fluctuations at residues 505–515 and 857–879, suggesting localized

Table 2. Docking Results of Alpelisib and α-Chaconine with Wild-type and Nonsynonymous Single Nucleotide Polymorphism of p110α

Ligand	Mutation	ΔG (kcal/mol)	Interacting Residues		
			H-bond	Hydrophobic	van der Waals
alpelisib	Wild type	-10.29	Lys802, Val851, Ser854, Gln859	Trp780, Ile800, Tyr836, Ile848, Val850, Met922, Ile932	Pro778, Lys802, Asn853, His855, Thr856
	E542K	-10.21	Val851, Ser854, Gln859	Met772, Pro778, Ile800, Lys802, Tyr 836, Val850, Met922, Ile932	Trp780, Tyr836, Ile848, Arg852, Asn853, His855, Thr856
	E545K	-10.38	Val851, Ser854, Gln859	Met772, Pro778, Ile800, Lys802, Tyr 836, Val850, Met922, Ile932	Trp780, Tyr836, Ile848, Arg852, Asn853, His855, Thr856
	H1047R	-10.27	Val851, Ser854, Gln859	Pro778, Trp780, Ile800, Lys802, Tyr836, Ile848, Val850, Met922, Phe930, Ile932	Met772, Glu849, Asn853, His855, Thr856, Asp933
CHA	Wild type	-8.36	Arg770, Ser773, Ser919, Asp933	Trp780, Arg852, Ile932	Ser774, Ala775, Glu798, Asn853, Ser854, His855, Thr856, Met858, Gln859, His917, Asn920, Met922,
	E542K	-8.55	Lys802, Asp810, Tyr836	Met772, Trp780, Ile848, Arg852, His855, Met922, Ile932	Arg770, Pro778, Leu807, Leu814, Val850, Val851, Asn853, Ser854, Thr856, Met858, Gln859, Ser874, His917, Ser919, Asn920, Asp933, Phe934
	E545K	-9.08	Ala775, Lys802, Tyr836	Trp780, Leu807, Arg852, His855, Met922	Arg770, Ser773, Ser774, Pro778, Asp810, Leu814, Thr856, Met858, Gln859, Ser919, Ile932, Asp933, Phe934, Glu798, Arg852, Asn853, Ser854, Val850, Val851, Ile848, Met772,
	H1047R	-9.93	Ser774, Lys802, Tyr836, Ser919, Asp933	Trp780, Leu807, Met772, Arg852, His855, Met922	Arg770, Ser773, Glu798, Asp810, Leu814, Ile848, Val850, Val851, Asn853, Ser854, Thr856, Met858, Gln859, Ile932, Phe934, Tyr836

Table 3. Molecular Mechanics Poisson–Boltzmann Surface Area Binding Free Energy Calculations of p110α-alpelisib and p110α-α-chaconine complexes from 100 nanoseconds molecular dynamics simulations (unit: kcal/mol)

Alpelisib				
Parameter	WT	*E542K*	*E545K*	*H1047R*
vdW	-44.6	-39.82	-44.46	-35.67
EEL	-23.76	-16.95	-27.03	-9.33
EPB	43.67	36.54	46.8	27.64
ENPOLAR	-4.52	-4.42	-4.47	-4.05
EDISPER	0	0	0	0
G_{gas}	-68.36	-56.78	-71.48	-45
G_{solv}	39.15	32.12	42.32	23.58
ΔG_{bind}	-29.21	-24.66	-29.16	-21.41
α-chaconine				
Parameter	WT	*E542K*	*E545K*	*H1047R*
vdW	-32.09	-47.19	-40.87	-47.99
EEL	-12.15	-15.97	-27.03	-40.47
EPB	31.6	50.9	50.56	68.79
ENPOLAR	-4.43	-5.89	-5.49	-6.22
EDISPER	0	0	0	0
G_{gas}	-44.24	-63.16	-67.91	-88.46
G_{solv}	27.17	45.02	45.07	62.57
ΔG_{bind}	-17.07	-18.15	-22.84	-25.88

conformational flexibility in these regions upon alpelisib binding to the *E542K* mutant (Figure 2C). Similarly, the CHA-*E545K* complex exhibited fluctuations in the 857–879 residue region. These patterns indicate that specific mutant-ligand combinations may induce regional instability in p110α, potentially affecting binding site integrity (Figure 2D). SASA and Rg analyses were conducted to assess the overall structural stability and compactness of all ligand-protein complexes throughout the simulation (Figure 2E–H). SASA values remained relatively stable across all complexes for both alpelisib and CHA, ranging approximately between 48,000 and 52,000 Å², indicating minimal changes in solvent exposure upon ligand binding (Figure 2E and 2F). Similarly, Rg values remained stable across all complexes, fluctuating within a narrow range of approximately 32.8–33.6 Å, confirming the preservation of overall protein compactness and structural integrity throughout the simulation (Figure 2G and 2H). MM-PBSA analysis was conducted to estimate the binding free energy of each ligand-protein complex. For alpelisib-p110α complexes, the wild-type exhibited the lowest binding energy (−29.21 kcal/mol), followed by *E545K* (−29.16 kcal/mol), *E542K* (−24.66 kcal/mol), and *H1047R* (−21.41 kcal/mol) (Table 3). For CHA-p110α complexes, the *H1047R* mutant showed the most favorable binding affinity (−25.88 kcal/mol), followed by *E545K* (−22.84 kcal/mol), *E542K* (−18.15 kcal/mol), and wild-type (−17.07 kcal/mol) (Table 3). Notably,

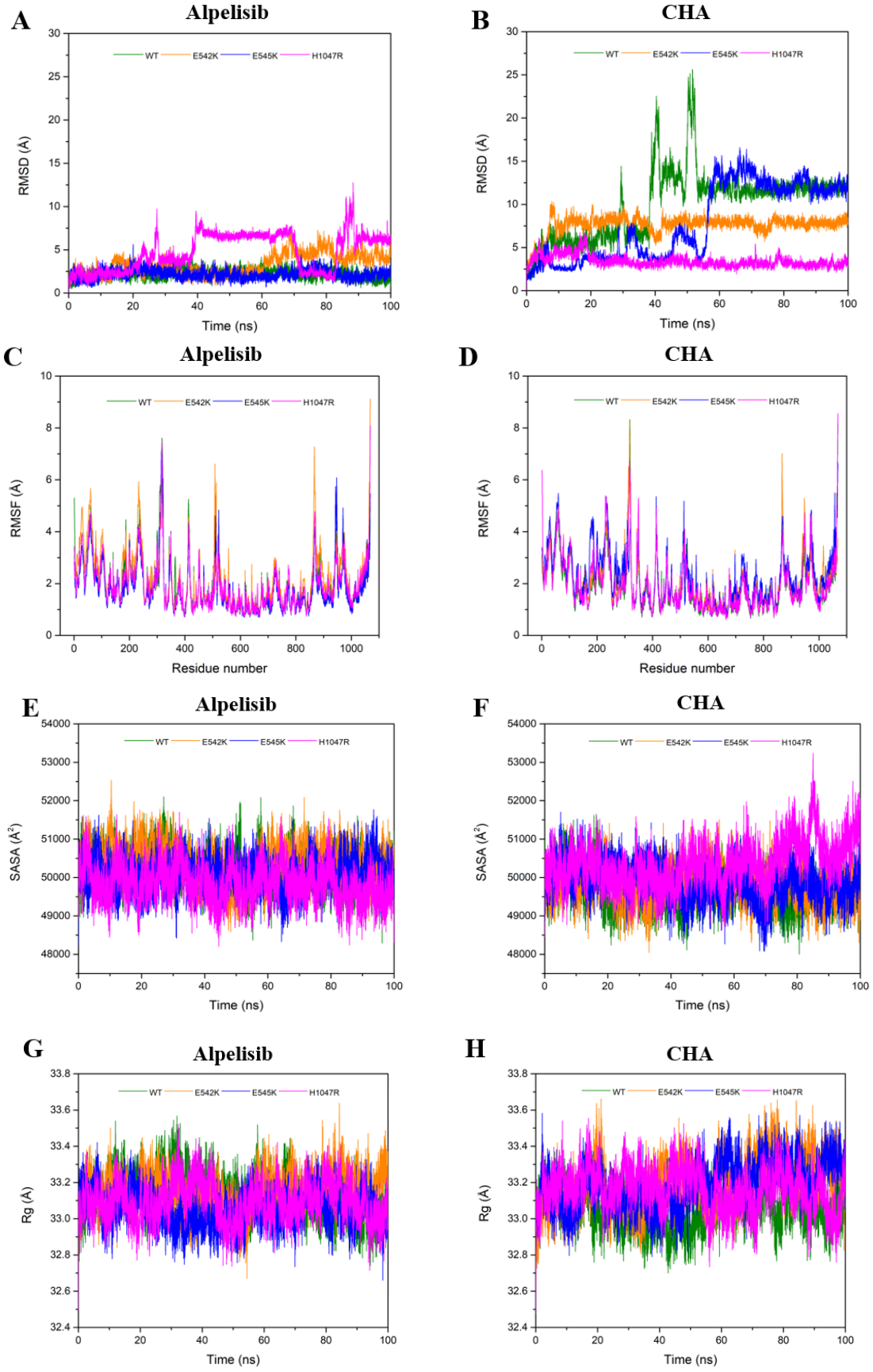

Figure 2. Molecular Dynamics Simulation Analysis of p110α Complexes Over 100 Nanoseconds. (A-B) Ligand-to-backbone root-mean-square deviation profiles for alpelisib and α-chaconine (CHA) complexes; (C-D) root-mean-square fluctuation analysis of residues in complexes with alpelisib and α-chaconine (CHA); (E-F) solvent- accessible surface area trajectories for alpelisib α-chaconine (CHA) complexes; and (G-H) radius of gyration profiles for alpelisib and α-chaconine (CHA) bound to wild-type (green), *E542K* (orange), *E545K* (blue), and *H1047R* (magenta) p110α variants.

CHA demonstrated a higher binding affinity for *H1047R* (−25.88 kcal/mol) compared to alpelisib (−21.41 kcal/mol), suggesting mutation-selective targeting potential.

Discussion

The purpose of this study was to assess CHA as a potential *PI3K* inhibitor targeting wild-type and mutant forms of p110α, a catalytic component of *PI3Kα*. A high frequency of *PIK3CA* mutations was identified from breast cancer studies in cBioPortal. The three most frequent hotspot mutations (*E542K*, *E545K*, and *H1047R*) were selected for further analysis. These findings are consistent with previously reported mutation patterns in breast cancer, highlighting their significant role in *PI3Kα* activation [25]. The wild-type and mutant p110α models were constructed using SWISS-MODEL and validated using PROCHECK and ERRAT webservers. All models showed more than 90% of residues in the most favored regions, indicating reliable structural quality for subsequent docking analysis [26]. These models were then used for molecular docking to evaluate interactions with the established *PI3K* inhibitor alpelisib and CHA using AutoDock 4.2. Alpelisib demonstrated relatively similar binding affinities across wild-type and mutant p110α models. The loss of the Lys802 hydrogen bond in alpelisib-mutant complexes may partially explain the reduced binding affinity observed in mutants, suggesting a structural basis for potential resistance to alpelisib in *PIK3CA*-mutant breast cancer. In contrast, CHA exhibited progressively stronger binding to mutant variants, particularly *H1047R*, suggesting favorable complementarity with mutation-induced conformational changes in the kinase domain mutations. Although CHA formed different hydrogen bonds with wild-type p110α, it established interactions with Lys802 in mutant complexes, similar to the key interaction observed in the wild-type p110α-alpelisib complex.

Molecular dynamics simulations further supported these observations. RMSD analysis demonstrated stable interactions of alpelisib with wild-type, *E542K*, and *E545K* mutants of p110α, but revealed conformational instability in the alpelisib-H1047R complex. These differential stability profiles suggest that the *H1047R*-induced conformational shift in the activation loop creates a binding environment particularly favorable for CHA. RMSF is a parameter used to evaluate the fluctuation of protein atoms relative to their reference positions over a given time frame. The absence of significant fluctuations at the key residue Lys802 across all complexes indicates preservation of binding site stability throughout the simulation. SASA analysis, which measures the extent of protein surface exposed to solvent, revealed comparable structural stability across all complexes. Similarly, Rg, which reflects the compactness of protein folding, remained consistent across all complexes [27]. Notably, both SASA and Rg analyses confirm that the observed variations in RMSD profiles are attributable to localized binding site dynamics rather than global structural changes, indicating overall structural compactness and stability. Furthermore, binding free energy analysis using the MM-PBSA method provided quantitative evidence of CHA's selectivity toward the *H1047R* mutant. Notably, CHA exhibited a more favorable binding energy for the *H1047R* mutant compared to alpelisib (ΔG = −25.88 vs −21.41 kcal/mol), indicating its potential utility in treating *H1047R*-associated breast cancers, particularly in patients with limited response to standard alpelisib treatment. Interestingly, this finding contrasts with the study by Mentes et al., which reported stable RMSD values for alpelisib across wild-type, *E542K*, *E545K*, and *H1047R* mutant *PI3Kα* [22], highlighting the importance of evaluating ligand-specific dynamics beyond docking scores alone.

The *PI3K* signaling pathway plays a crucial role in cellular metabolism, growth, survival, cell cycle regulation, and migration. Overactivation of *PI3K* in BCSCs contributes to drug resistance and metastasis. *PIK3CA* encodes the p110α subunit of *PI3Kα*, and its mutations enhance *PI3K* activity [25, 28]. Helical domain mutations (*E542K* and *E545K*) disrupt p110α-p85α interactions, leading to significant conformational alterations [29, 30], whereas the kinase domain mutation *H1047R* directly alters the activation loop conformation [31]. These structural consequences underscore the importance of targeting mutation-specific conformations, particularly *H1047R*, for effective BCSC-targeted therapy.

In conclusion, this computational study suggests that CHA is a promising selective *PI3K* inhibitor for the *H1047R PIK3CA* mutant, supporting its potential application in personalized breast cancer therapy. A comparable approach has been reported in studies targeting thymidine phosphorylase, where berbamine showed lower binding affinity than 5-fluorouracil, demonstrating the broader applicability of natural compound-based inhibitor discovery [30]. However, this study is limited to computational analyses and lacks experimental validation in BCSC models, especially the 3D model. As a preliminary computational study, further experimental validation is required to verify these findings. Future research should investigate the cytotoxic activity of CHA in both 2D monolayer and 3D BCSC models. Additionally, validation using an engineered *H1047R PI3Kα* mutant enzyme assay is necessary to confirm the inhibitory effect of CHA on *H1047R PI3Kα* activity and support its development as a mutation-specific therapeutic for *H1047R*-positive breast cancer. These experimental steps are essential to bridge the gap between the current computational predictions and preclinical application.

Author Contribution Statement

BWS: writing (original manuscript), formal analysis, data curation, and conceptualization. NSOU: Supervision, Validation, and Formal Analysis. BSR: Resources and Formal Analysis. RSA: Resource and Software. AS: Supervision. AH: Writing - review and editing, supervision, methodology, and conceptualization.

Acknowledgements

General

The authors would like to thank the Laboratory of Medicinal Chemistry, Faculty of Pharmacy, Gadjah Mada University for facilitating the MD simulations.

Funding Statement

This research was funded by the Ministry of Education, Culture, Research, and Technology (Kemdikbudristek), Republic of Indonesia, through Penelitian Tesis Magister 2025, grant number 2652/UN1/DITLIT/Dit-Lit/PT.01.03/2025.

Data Availability

The data utilized to support the results of this research are available upon reasonable request from the author.

Conflict of Interest

The authors have no conflicts of interest to declare.

References

1. Wang J, Wu SG. Breast cancer: An overview of current therapeutic strategies, challenge, and perspectives. Breast Cancer (Dove Med Press). 2023;15:721-30. https://doi.org/10.2147/bctt.S432526.
2. Ramos P, Bentires-Alj M. Mechanism-based cancer therapy: Resistance to therapy, therapy for resistance. Oncogene. 2015;34(28):3617-26. https://doi.org/10.1038/onc.2014.314.
3. Hen O, Barkan D. Dormant disseminated tumor cells and cancer stem/progenitor-like cells: Similarities and opportunities. Semin Cancer Biol. 2020;60:157-65. https://doi.org/10.1016/j.semcancer.2019.09.002.
4. Ibrahim SA, Gadalla R, El-Ghonaimy EA, Samir O, Mohamed HT, Hassan H, et al. Syndecan-1 is a novel molecular marker for triple negative inflammatory breast cancer and modulates the cancer stem cell phenotype via the il-6/stat3, notch and egfr signaling pathways. Mol Cancer. 2017;16(1):57. https://doi.org/10.1186/s12943-017-0621-z.
5. Takebe N, Harris PJ, Warren RQ, Ivy SP. Targeting cancer stem cells by inhibiting wnt, notch, and hedgehog pathways. Nat Rev Clin Oncol. 2011;8(2):97-106. https://doi.org/10.1038/nrclinonc.2010.196.
6. Miricescu D, Totan A, Stanescu S, II, Badoiu SC, Stefani C, Greabu M. *PI3K/Akt*/mtor signaling pathway in breast cancer: From molecular landscape to clinical aspects. Int J Mol Sci. 2020;22(1). https://doi.org/10.3390/ijms22010173.
7. Alves CL, Ehmsen S, Terp MG, Portman N, Tuttolomondo M, Gammelgaard OL, et al. Co-targeting cdk4/6 and akt with endocrine therapy prevents progression in cdk4/6 inhibitor and endocrine therapy-resistant breast cancer. Nat Commun. 2021;12(1):5112. https://doi.org/10.1038/s41467-021-25422-9.
8. Wilhoit T, Patrick JM, May MB. Alpelisib: A novel therapy for patients with *PIK3CA*-mutated metastatic breast cancer. J Adv Pract Oncol. 2020;11(7):768-75. https://doi.org/10.6004/jadpro.2020.11.7.9.
9. Turner NC, Im SA, Saura C, Juric D, Loibl S, Kalinsky K, et al. Inavolisib-based therapy in *PIK3CA*-mutated advanced breast cancer. N Engl J Med. 2024;391(17):1584-96. https://doi.org/10.1056/NEJMoa2404625.
10. Lopez S, Schwab CL, Cocco E, Bellone S, Bonazzoli E, English DP, et al. Taselisib, a selective inhibitor of *PIK3CA*, is highly effective on *PIK3CA*-mutated and her2/neu amplified uterine serous carcinoma in vitro and in vivo. Gynecol Oncol. 2014;135(2):312-7. https://doi.org/10.1016/j.ygyno.2014.08.024.
11. Nunnery SE, Mayer IA. Management of toxicity to isoform α-specific *PI3K* inhibitors. Ann Oncol. 2019;30(Suppl_10):x21-x6. https://doi.org/10.1093/annonc/mdz440.
12. Yang SA, Paek SH, Kozukue N, Lee KR, Kim JA. Alpha-chaconine, a potato glycoalkaloid, induces apoptosis of ht-29 human colon cancer cells through caspase-3 activation and inhibition of erk 1/2 phosphorylation. Food Chem Toxicol. 2006;44(6):839-46. https://doi.org/10.1016/j.fct.2005.11.007.
13. Hermawan A, Pamungkas Putri DD, Fatimah N, Rhamandana Putra IM, Lestari IA. A-chaconine increases the sensitivity of her2+ breast cancer cells to trastuzumab by targeting acetylcholinesterase. Comput Biol Med. 2025;188:109809. https://doi.org/10.1016/j.compbiomed.2025.109809.
14. Shih YW, Chen PS, Wu CH, Jeng YF, Wang CJ. Alpha-chaconine-reduced metastasis involves a *PI3K/Akt* signaling pathway with downregulation of nf-kappab in human lung adenocarcinoma a549 cells. J Agric Food Chem. 2007;55(26):11035-43. https://doi.org/10.1021/jf072423r.
15. Karaboğa Arslan AK, Yerer MB. A-chaconine and α-solanine inhibit rl95-2 endometrium cancer cell proliferation by reducing expression of akt (ser473) and erα (ser167). Nutrients. 2018;10(6). https://doi.org/10.3390/nu10060672.
16. Kulshreshtha S, Chaudhary V, Goswami GK, Mathur N. Computational approaches for predicting mutant protein stability. J Comput Aided Mol Des. 2016;30(5):401-12. https://doi.org/10.1007/s10822-016-9914-3.
17. Shukla r, tripathi t. Molecular dynamics simulation of protein and protein–ligand complexes. Comput. Drug des., singapore: Springer singapore; 2020, p. 133–61. Https://doi.Org/10.1007/978-981-15-6815-2_7.
18. Pejaver V, Urresti J, Lugo-Martinez J, Pagel KA, Lin GN, Nam HJ, et al. Inferring the molecular and phenotypic impact of amino acid variants with mutpred2. Nat Commun. 2020;11(1):5918. https://doi.org/10.1038/s41467-020-19669-x.
19. Bora s, kukreti r, hasija y. An in-silico analysis predicting the impact of coding single nucleotide polymorphisms (snps) in the human multidrug pump abcg2. Hum gene 2023;38:201213. Https://doi.Org/10.1016/j.Humgen.2023.201213.
20. Waterhouse A, Bertoni M, Bienert S, Studer G, Tauriello G, Gumienny R, et al. Swiss-model: Homology modelling of protein structures and complexes. Nucleic Acids Res. 2018;46(W1):W296-w303. https://doi.org/10.1093/nar/gky427.
21. Laskowski R, Macarthur MW, Moss DS, Thornton J. Procheck: A program to check the stereochemical quality of protein structures. Journal of Applied Crystallography. 1993;26:283-91. https://doi.org/10.1107/S0021889892009944.
22. Colovos C, Yeates TO. Verification of protein structures: Patterns of nonbonded atomic interactions. Protein Sci. 1993;2(9):1511-9. https://doi.org/10.1002/pro.5560020916.
23. Menteş M, Karakuzulu BB, Uçar GB, Yandım C. Comparative molecular dynamics analyses on *PIK3CA* hotspot mutations with *PI3Kα* specific inhibitors and atp. Comput Biol Chem. 2022;99:107726. https://doi.org/10.1016/j.compbiolchem.2022.107726.
24. Camargo PG, da Silva RB, Zuma AA, Garden SJ, Albuquerque MG, Rodrigues CR, et al. In silico evaluation of n-aryl-1,10-phenanthroline-2-amines as potential inhibitors of t. Cruzi gp63 zinc-metalloprotease by docking and

molecular dynamics simulations. Sci Rep. 2025;15(1):6036. https://doi.org/10.1038/s41598-025-90088-y.
25. Martínez-Sáez O, Chic N, Pascual T, Adamo B, Vidal M, González-Farré B, et al. Frequency and spectrum of *PIK3CA* somatic mutations in breast cancer. Breast Cancer Res. 2020;22(1):45. https://doi.org/10.1186/s13058-020-01284-9.
26. Sobolev OV, Afonine PV, Moriarty NW, Hekkelman ML, Joosten RP, Perrakis A, et al. A global ramachandran score identifies protein structures with unlikely stereochemistry. Structure. 2020;28(11):1249-58.e2. https://doi.org/10.1016/j.str.2020.08.005.
27. Kushwaha PP, Singh AK, Bansal T, Yadav A, Prajapati KS, Shuaib M, et al. Identification of natural inhibitors against sars-cov-2 drugable targets using molecular docking, molecular dynamics simulation, and mm-pbsa approach. Front Cell Infect Microbiol. 2021;11:730288. https://doi.org/10.3389/fcimb.2021.730288.
28. Bai X, Ni J, Beretov J, Graham P, Li Y. Cancer stem cell in breast cancer therapeutic resistance. Cancer Treat Rev. 2018;69:152-63. https://doi.org/10.1016/j.ctrv.2018.07.004.
29. Yu J, Zhang Y, McIlroy J, Rordorf-Nikolic T, Orr GA, Backer JM. Regulation of the p85/p110 phosphatidylinositol 3'-kinase: Stabilization and inhibition of the p110alpha catalytic subunit by the p85 regulatory subunit. Mol Cell Biol. 1998;18(3):1379-87. https://doi.org/10.1128/mcb.18.3.1379.
30. Zhao L, Vogt PK. Helical domain and kinase domain mutations in p110alpha of phosphatidylinositol 3-kinase induce gain of function by different mechanisms. Proc Natl Acad Sci U S A. 2008;105(7):2652-7. https://doi.org/10.1073/pnas.0712169105.
31. Huang CH, Mandelker D, Schmidt-Kittler O, Samuels Y, Velculescu VE, Kinzler KW, et al. The structure of a human p110alpha/p85alpha complex elucidates the effects of oncogenic *PI3K*alpha mutations. Science. 2007;318(5857):1744-8. https://doi.org/10.1126/science.1150799.